



Mechanical synthesis of nanostructured $Y_2Ti_2O_7$ pyrochlore oxides

E. Simondon^a, P.-F. Giroux^{a,*}, L. Chaffron^a, A. Fitch^b, P. Castany^c, T. Gloriant^c

^a DEN-Service de Recherches Métallurgiques Appliquées, CEA, Université Paris-Saclay, F-91191, Gif-sur-Yvette, France

^b ESRF-The European Synchrotron Radiation Facility, CS40220, 38043, Grenoble, France

^c Univ Rennes, INSA Rennes, UMR CNRS 6226 ISCR, 35000, Rennes, France

ARTICLE INFO

Keywords:

Pyrochlore oxide
Mechanical milling
Nanostructure
X-ray diffraction (XRD)
Synchrotron radiation

ABSTRACT

Pyrochlore-type $Y_2Ti_2O_7$ powders were successfully synthesized by mechanical milling. Nanosized powders of Y_2O_3 and TiO_2 are milled to form an amorphous mixture of $Y_2Ti_2O_7$ containing a small quantity of crystallized fluorite structure and initial constituents. The desired fully crystallized pyrochlore phase is obtained from this mixture through heat treating at 900 °C. In situ X-ray Diffraction by Synchrotron radiation investigations reveal that this transformation takes place through a first step of crystallization into a fluorite-like structure at 800 °C. The formation of the pyrochlore structure occurs around 900 °C. The obtained product is a nanostructured pyrochlore powder of which can be integrated in the manufacturing process of oxide dispersion strengthened steels.

1. Introduction

$Y_2Ti_2O_7$ oxides are part of a large family of $A_2B_2O_7$ oxides displaying pyrochlore structure, where A and B are metal cations. The fully ordered pyrochlore structure presents a cubic symmetry (Space Group: $Fd\bar{3}m$) and can be described in terms of a superstructure of the ideal defect fluorite structure (cubic, S.G. $Fm\bar{3}m$) with twice the cell constant ($a \approx 10 \text{ \AA}$) [1].

In this study, $Y_2Ti_2O_7$ pyrochlore oxides are produced and examined to be directly introduced in Oxide Dispersion Strengthened (ODS) steel during manufacturing process. The presence of a dense dispersion of this highly stable oxide under irradiation in the ferritic matrix improves mechanical strength and traps irradiation defects [2] [3].

$Y_2Ti_2O_7$ is usually produced by a standard solid state process. This method requires repeated cycles of ball-milling and heat treatments above 1000 °C, involving an important growth and aggregation of particles [4] [5]. Among the solid state processes, high-energy ball milling has revealed to be an efficient method to produce complex oxide nanopowders [6] [7] [8]. It has been demonstrated that the process involving repeated ball-powder collision events during the milling could induce mechanochemical solid-state reactions in the milled powder [9] [10]. The repeated welding and fracturing of powder particles increases the area of contact between the reactant powder particles and allows fresh surfaces to come into contact repeatedly. As a consequence, the reaction that normally requires high temperatures to facilitate the diffusion occurs at room temperature during mechanical

milling and nanosized particles can be obtained [11].

$Y_2Ti_2O_7$ pyrochlore powders have recently been produced by a simple mechanochemical synthesis technique [12] [13] [14]. Moreno et al. [12] showed that a milling of a stoichiometric mixture of Y_2O_3 and TiO_2 powders for 19 h in a zirconia planetary ball mill leads to obtaining a single-phased powder. Fuentes et al. [13] and Singh et al. [14] showed that the produced as-milled powders were composed by partially disordered phases, which are intermediate between the ordered pyrochlore and disordered fluorite structures. This partially disordered pyrochlore structure transforms into the ordered form around 800 °C, mainly due to oxygen re-arrangements [13].

The aim of this contribution is to propose a mechanochemical method to synthesize highly pure $Y_2Ti_2O_7$ powders with an ordered pyrochlore type of structure and nanosized crystallites. After a first step of milling of the initial constituents, a short annealing allows the transformation into the fully ordered pyrochlore phase while limiting the crystallites growth.

2. Materials and methods

Initial powders used in this work were nano-sized TiO_2 (Degussa, 99,5%) and Y_2O_3 (Sigma-Aldrich, 99,9%) powders. They were pelletized into an 8-mm-diameter die under 3 tonnes mass and then submitted to a primary annealing for 10 h under vacuum (10^{-6} mbar at 550 °C and 1000 °C respectively, in order to remove adsorbed H_2O). Appropriate amount of the as-treated constituent oxides was selected

* Corresponding author.

E-mail address: pierre-francois.giroux@cea.fr (P.-F. Giroux).

($Y_2O_3/2TiO_2$) to reach a complete transformation in $Y_2Ti_2O_7$. Batches of 3 g were ball milled in a modified FRITSCH Pulverisette-0 mill with tungsten carbide vial and ball under a static vacuum (10^{-6} mbar) for 120 h with an intensity of $1400 \text{ m}\cdot\text{s}^{-2}$ [15]. Heat treatments on the as-milled powders were performed under vacuum (10^{-6} mbar) at 900°C with a $10^\circ\text{C}\cdot\text{min}^{-1}$ temperature ramp followed by an immediate natural cooling. From the first heat treatment of the initial powders to the harvesting of milled and annealed final powders, the samples were at all time handled in a controlled atmosphere (argon or vacuum) in order to prevent any interaction with air. The samples were characterized by X-ray powder diffraction, using a BRUKER D8 diffractometer with Ni-filtered $\text{CuK}\alpha_1$ radiation ($\lambda = 1.5406 \text{ \AA}$). The diffraction patterns of the samples were measured over the angular range $13\text{--}70^\circ$ (2θ) with step size 0.02° and scan speed $0.24^\circ\cdot\text{min}^{-1}$. The samples were also examined by thermal analysis in a SETARAM TAG 24 using a typical sample mass of 100 mg and a heating rate of $10^\circ\text{C}\cdot\text{min}^{-1}$ in argon or air. In situ XRD spectra were collected on beam line ID22 (using $\lambda = 0.495992 \text{ \AA}$ wavelength) at the European Synchrotron Radiation Facility (ESRF, Grenoble, France). The scans were performed at $10^\circ\cdot\text{min}^{-1}$ from 5 to 20° (2θ) of the central detector, with a 0.5 mm silica-glass capillary, $10 \mu\text{m}$ wall thickness, spun axially at 787 rpm . The temperature ramp of $10 \text{ K}\cdot\text{min}^{-1}$ was achieved via a hot-air blower. Scanning electron microscopy (SEM) was carried out on a HIROX SH-3500MB microscope working at 20 kV . Transmission electron microscopy (TEM) and selected area electron diffraction (SAED) were performed on a JEOL 2100 working at 200 keV .

3. Results

Fig. 1(a) shows the evolution of the XRD pattern of the $Y_2O_3 + 2TiO_2$ mixture before and after the milling in a high energy ball

mill. As a reference, the XRD pattern of the starting mixture (Fig. 1(a)(i)) presents peaks from both cubic Y_2O_3 (ICDD card 00-41-1105) and TiO_2 in the form of rutile (01-089-0553) and anatase (00-021-1272). The XRD diffraction pattern of the ball-milled powder (Fig. 1(a)(ii)) indicates that the powder is mostly amorphous-like with broad peaks of low intensities and contains a crystalline fraction indicated by a few narrow peaks of low intensity. The decrease in intensity and increase in peak broadening is the result of, on the one hand, a considerable refinement of particle and crystallite size and, on the other hand, the introduction of a large number of structural defects in the constituent oxides. The diffraction pattern is then decomposed into a baseline (Fig. 1(a)(iii)) representing the amorphous component and the deconvolved signal (Fig. 2(a)(iv)) representing the crystalline fraction. On the baseline pattern (Fig. 1(a)(iii)), the main broad peak roughly correspond to the (222) main reflections of $Y_2Ti_2O_7$ at $2\theta = 30.64^\circ$. On the deconvolved signal (Fig. 1(a)(iv)), the main reflections of anatase TiO_2 and cubic Y_2O_3 are evident, revealing the presence of residual initial constituents.

SEM observations reveal that after the milling, the powder is characterized by a typical morphology of ball-milled ceramic samples composed by sub-micronic agglomerated particles of irregular shape [16] (Fig. 1(b)). They are themselves constituted of nanoparticles agglomerates (Fig. 1(c)). The microstructure of this milled powder was characterized by TEM and SAED. Fig. 2(a) and (b) present observation zones at the edge of two different agglomerates, in bright (Fig. 2(a)) or dark field (Fig. 2(b)) with the associated SAED patterns. In most observed agglomerates, even the diffraction contrast in the micrograph fails to reveal any crystallite within the powder particle, as illustrated in Fig. 2(b). The corresponding SAED diagram presents a very diffuse ring along with some scattered bright spots. The diffuse maxima observed can be explained as a result of small domain size together with poor

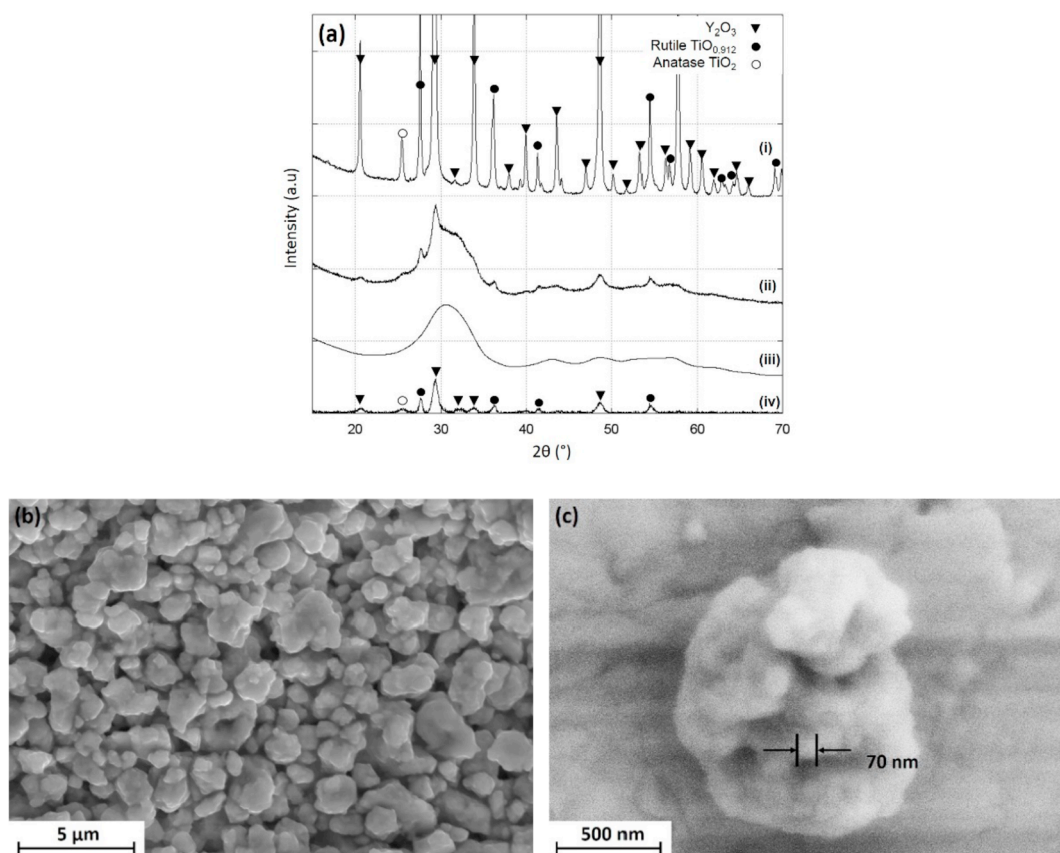


Fig. 1. (a) X-ray diffraction patterns of the starting mixture (i) and the ball-milled powder (ii). The diffractogram (ii) is decomposed in a baseline representing the amorphous component (iii) and the deconvolved signal representing crystalline fractions (iv). (b) and (c) are SEM micrographs of the ball-milled powder at different magnifications.

Download English Version:

<https://daneshyari.com/en/article/11026721>

Download Persian Version:

<https://daneshyari.com/article/11026721>

[Daneshyari.com](https://daneshyari.com)